Journal of Structural Geology 33 (2011) 537–550

Contents lists available at ScienceDirect

Journal of Structural Geology

journal homepage: www.elsevier.com/locate/jsg

Grainsize evolution in ductile shear zones: Implications for strain localization and the strength of the lithosphere

J.P. Platt*, W.M. Behr

Department of Earth Sciences, University of Southern California, Los Angeles, CA 90089, USA

ARTICLE INFO

Article history:
Received 12 July 2010
Received in revised form
2 January 2011
Accepted 29 January 2011
Available online 25 February 2011

Keywords:
Rheology
Grainsize
Shear zone
Strain localization

ABSTRACT

At high stresses and low temperatures, grainsize reduction by dynamic recrystallization profoundly modifies rock rheology. Strain energy driven grain-boundary migration (ρGBM) is involved both in the nucleation of new grains by the grain-boundary bulging mechanism (BLG), and in the subsequent evolution of the microstructure. Above the D_{min} line, which is a line in stress/grainsize space that defines the minimum size of nucleus that can form by BLG, ρGBM dominates the microstructure, and grain growth by surface energy driven grain-boundary migration (γGBM) is inhibited. The recrystallized grainsize is therefore dominated by the nucleation process, possibly controlled by the size of subgrains or dislocation cells within the old grains. This provides a first-order explanation for the experimentally observed grainsize-stress relationship.

ρGBM is an important agent of recovery in rocks deformed by dislocation creep, sweeping out dislocations and counteracting work-hardening. We have derived a new flow law (DRX-assisted dislocation creep) based on this process, which exhibits grainsize sensitivity as a result of the role of ρGBM. If grainsize obeys the empirically-determined grainsize-stress relationship, DRX creep has an effective stress exponent of a little over 4, consistent with experimental observations and inferences from naturally deformed rocks. DRX creep may be an important agent in weakening quartz at low temperatures, whereas current flow law data suggest it may not be important in olivine.

Rocks deformed and dynamically recrystallized above the D_{min} line may switch from climb-assisted dislocation creep to grainsize-sensitive creep (Coble creep, DRX creep, or creep dominated by grain-boundary sliding), resulting in weakening. Lithospheric-scale shear zones are likely to evolve at approximately constant stress; under these conditions weakening results in an increase in strain rate, not a stress drop. The rate of dislocation motion, the dislocation density, and the dynamically recrystallized grainsize all remain the same, and grain growth will be inhibited by the activity of ρGBM. Hence the switches in deformation mechanism and the weakening they cause will be permanent, so long as the tectonic boundary conditions remain unchanged. Grainsize reduction caused by dynamic recrystallization may therefore play a fundamental role in lithospheric weakening, and may be a key process in the maintenance of plate tectonics.

1. Introduction

The processes that cause localization of strain in the lithosphere are fundamental to our understanding of plate tectonics: numerical models of mantle convection fail to reproduce plate-like behavior in the thermal boundary layer unless the material shows a significant degree of strain localization (Bercovici, 2003; Tackley, 2000). Current flow laws describing deformation in the ductile field do not inherently predict strain localization, however: power-law and exponential creep laws all predict a positive relationship between stress and strain rate, which will tend to distribute deformation rather than localize it. Mantle convection models that invoke plate-like behavior commonly do so either by prescribing zones of weakness (Zhong and Gurnis, 1996) or by imposing a plastic yield strength for the deforming material (Trompert and Hansen, 1998).

A number of processes have been suggested that could explain weakening and strain localization in ductile shear zones, including dissipative heating (e.g., Regenauer-Lieb et al., 2006), phase changes (Brodie and Rutter, 1987; Tingle et al., 1993; White and Knipe, 1978), development of lattice preferred orientations (Poirier, 1980), and grainsize reduction by cataclasis or dynamic recrystallization (Handy et al., 2007). All of these mechanisms have

* Corresponding author. Tel.: +1 213 821 1194.
E-mail addresses: jplatt@usc.edu (J.P. Platt), behr@usc.edu (W.M. Behr).

0191-8141/$ – see front matter © 2011 Elsevier Ltd. All rights reserved.
doi:10.1016/j.jsg.2011.01.018

the potential to weaken rocks and hence localize strain, but the almost universal association of grainsize reduction with ductile shear zones suggests to us that dynamic recrystallization is one of the most potent, and we therefore need an improved understanding of the microphysical processes involved. In particular, grainsize reduction associated with dynamic recrystallization can cause weakening by increasing the rates of both grain-boundary sliding and grain-boundary diffusion creep (Drury, 2005; Jaroslow et al., 1996; Jin et al., 1998; Rutter, 1995; Warren and Hirth, 2006), and by facilitating the ingress of water and thereby enhancing hydration reactions and the hydrolytic weakening of crystal lattices (Tullis et al., 1996). Grain-boundary migration associated with dynamic recrystallization may counteract work-hardening during dislocation creep (Fliervoet and White, 1995; Tullis and Yund, 1982, 1985), and could therefore result in significant changes in the flow laws relating stress and strain rate in the material. Most recent studies however, describe dynamic recrystallization in terms of a balance between grainsize reduction and grain growth (Braun et al., 1999; De Bresser et al., 2001; Hall and Parmentier, 2003; Montési and Hirth, 2003; Montési and Zuber, 2002). In this scenario, grain growth counteracts the weakening effect of grainsize reduction, which has led to the conclusion that dynamic recrystallization cannot lead to permanent strain localization under most circumstances (e.g., De Bresser et al., 2001). This conclusion is at odds with the clear association between localized shear zones and drastic grainsize reduction (Rutter and Brodie, 1988).

The purpose of this paper is to re-examine the mechanisms of dynamic recrystallization and the processes that control grainsize evolution during deformation. We conclude that dynamic recrystallization can act as a powerful recovery mechanism during low temperature dislocation creep, and we derive a new grainsize-sensitive flow law based on this concept, which may explain some of the experimental observations for grainsize sensitivity during dislocation creep. We also show that under the high stress, low temperature conditions that favor this mechanism, grain growth is inhibited. Grainsize reduction caused by dynamic recrystallization will therefore be irreversible unless the external boundary conditions change. Under these conditions, deformation mechanism switches resulting from grainsize reduction will be permanent, and will result in major rheological weakening. We discuss the implications of these conclusions for the use of dynamically recrystallized grainsize as an indicator of paleostress, and we place them in the context of the effect of shear zone development on the mechanics of plate boundaries.

2. Mechanisms of dynamic recrystallization

Naturally and experimentally deformed minerals and metals commonly show the development of new grains during dislocation creep, which are in general finer-grained than those in the undeformed aggregate. These new grains appear to form in response to plastic deformation induced by the motion of dislocations in the crystal lattice, and may be related to both work-hardening and recovery processes. If they are formed during deformation, the process is known as dynamic recrystallization. There is a general acceptance that the mean diameter of the new grains D_r is inversely related to the flow stress in the deforming medium by:

$$\frac{D_r}{b} = K_r\left(\frac{\sigma}{\mu}\right)^{-p} \quad (1)$$

where μ is the shear modulus, b is the Burgers vector (the lattice offset associated with an individual dislocation), K_r is a material parameter, and the exponent p lies in the range 0.6–2.0 (Poirier, 1985; Shimizu, 2008). Twiss (1977) calibrated this relationship using experimental data on metals and minerals, to obtain an average value for p of 1.47 ± 0.04. A relationship of this form has been generally confirmed by later experimental work on silicates: van der Wal et al. (1993) obtained a value for $p = 1.33 \pm 0.09$ on olivine, and Stipp and Tullis (2003) obtained $p = 1.26 \pm 0.13$ for quartz. The theoretical explanation advanced by Twiss (1977), however, was based on a non-physical mechanism for the formation of new grains (Poirier, 1985; Shimizu, 2008). Current explanations are mainly couched in terms of an interplay between grainsize reduction processes and grain growth (e.g., Derby and Ashby, 1987; Shimizu, 1998; De Bresser et al., 1998; Austin and Evans, 2007).

Various mechanisms have been proposed for dynamic recrystallization, and for a given material these may be controlled by stress, strain rate, and temperature, among other variables. The different mechanisms produce different microstructures (Stipp et al., 2010), and may lead to different relationships between stress and D_r (Shimizu, 2008). An experimental study by Hirth and Tullis (1992) defined three recrystallization regimes in quartz, dependent on temperature, strain rate, and water content, and characterized by distinct microstructures and mechanisms of dynamic recrystallization. *Regime 1*, occurring at the highest strain rates or the lowest temperatures, is characterized by the absence of microstructures (such as subgrains) indicating intracrystalline recovery processes facilitated by dislocation climb. Limited recrystallization takes place along pre-existing grain boundaries, caused by the small-scale migration or "bulging" of these boundaries. This process is driven by variations of dislocation density, and hence elastic strain energy, on either side of the boundary. Bulging produces small domains of dislocation-free lattice along the boundary, which tend to separate from their parent grains and define new grains. The old grains are work-hardened and show relatively little strain; the new grains have lower dislocation densities, and accommodate much of the deformation. *Regime 2*, at intermediate strain rate and temperature, is characterized by recrystallization both within and at the boundaries of grains by the process of sub-grain rotation, whereby the accumulation of dislocations into sub-grain walls increases the angular mismatch between the subgrains and the host grains until their walls can no longer be described in terms of a dislocation structure. The resulting new grains therefore start out with roughly the same size as the subgrains showing the largest angular mismatches. New grains and old grains have similar dislocation densities, and the old grains become strongly deformed. *Regime 3*, at low strain rate and high temperature, is characterized by a combination of rotation recrystallization and large scale grain-boundary migration. Recrystallization is pervasive, and the old grains disappear.

The microstructural regimes defined experimentally by Hirth and Tullis (1992) may not correspond precisely to those found in naturally deformed rocks (Stipp et al., 2002a), but it is now generally accepted that there are at least three mechanisms that contribute to recrystallization: small-scale bulging of grain boundaries (BLG); sub-grain rotation (SGR); and migration of grain boundaries on a relatively large scale, driven by some combination of strain energy and surface energy, which we refer to here as GBR. In the next three sections we discuss the implications of these different mechanisms of dynamic recrystallization for rheology and grainsize-stress relationships.

2.1. Recrystallization by BLG

The BLG mechanism is driven primarily by variations in dislocation density within adjacent grains, so that the grain-boundary migrates in the direction of greater dislocation density (Sakai, 1989) (Fig. 1a). This mechanism is favored under conditions of high stress

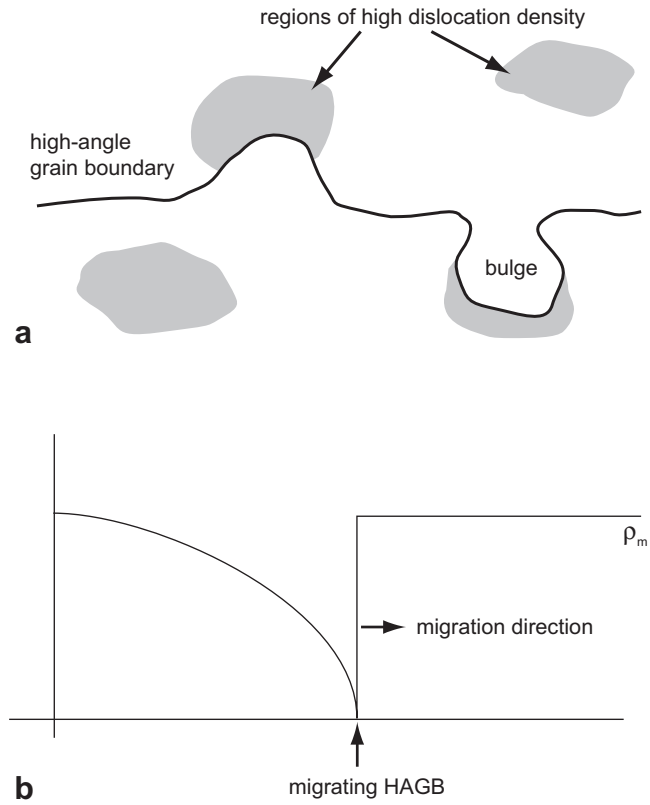

Fig. 1. a) High-angle grain-boundary showing bulges due to migration into regions of high dislocation density in the adjacent grain. Boundaries can migrate in either direction. b) Evolution of dislocation density distribution behind a migrating grain-boundary (after Humphreys and Hatherly, 2004). Dislocation density in the grain being consumed (right) has a value approximating the mean steady state value ρ_m in the aggregate. Density in the growing grain (left) increases from near zero at the boundary to the mean value at a some distance behind it. The new grain is weak, so the strain-rate, and hence the rate of dislocation multiplication, is initially high; both decrease with distance and increasing work-hardening away from the boundary.

and low temperature, limited intracrystalline recovery, and high dislocation density, and is dominant during experimental Regime 1 of Hirth and Tullis (1992). The growth of a bulge in the grain-boundary represents a net increase in grain-boundary area, which will be accompanied by an increase in surface energy. This is only possible if the reduction of lattice strain energy produced by the sweeping out of the dislocations in the area of the bulge is greater than the increase in surface energy, which leads to a criterion for the minimum size for a bulge (Derby and Ashby, 1987; Humphreys and Hatherly, 2004). If the energy per unit volume associated with dislocations is E_d, and the surface energy per unit area is γ, then for a bulge with radius r, the total energy E changes with r as:

$$\frac{dE}{dr} = 8\pi r\gamma - 4\pi r^2 E_d$$

Hence for $dE/dr \leq 0$,

$$r_{\min} = 2\gamma/E_d \tag{2}$$

E_d depends on the dislocation density ρ (e.g., Shimizu, 2008):

$$E_d = \frac{\rho\mu b^2\chi}{4\pi}\ln\frac{\beta}{2b\sqrt{\rho}} \tag{3}$$

where β is typically 3–4, and χ is a geometrical factor that varies between 1 for a screw dislocation and $1/(1-\nu)$ for an edge dislocation (ν is Poisson's ratio).

Grain-boundary bulges form in response to local variations in dislocation density, but once a bulge has consumed a local region of high ρ, its survival will depend on the mean value of ρ in the aggregate. If its radius is below the minimum value specified by Eq. (2) and (3) for the mean value of ρ, it will eventually shrink and disappear. During dislocation creep the mean dislocation density is related to flow stress by:

$$\rho = \left(\frac{\sigma}{\alpha\mu b}\right)^2 \tag{4}$$

where α is a geometrical constant of order unity. Hence

$$E_d = \frac{\sigma^2\chi\ln(\alpha\mu\beta/2\sigma)}{4\pi\mu\alpha^2} \tag{5}$$

The minimum diameter $D_{\min}$ of a nucleus formed by BLG is therefore related to the flow stress by:

$$D_{\min} = \frac{16\gamma\pi\mu\alpha^2}{\sigma^2\chi\ln(\alpha\mu\beta/2\sigma)} \tag{6}$$

Eq. (6) predicts an approximately inverse square relationship between the minimum size of a nucleus formed by BLG and the flow stress, and hence does not provide an explanation for the experimentally observed value of p. It does, however, separate a region in stress-grainsize space in which the BLG nucleation mechanism can operate from one in which it cannot. We explore alternative controls on the size of nuclei produced by BLG and the subsequent grainsize evolution in a later section.

2.2. Recrystallization by SGR

The SGR mechanism depends on the activity of climb-assisted recovery, which allows dislocations to organize themselves into sub-grain walls with relatively low strain energy. As dislocations continue to accumulate in the sub-grain walls, the angular mismatch increases, resulting in a rotation of the sub-grain relative to its surroundings. The angular mismatch may reach 10–15°, depending on the material, before the wall loses a structure that can be defined in terms of dislocations in a crystal lattice, and undergoes a transition to the amorphous structure characteristic of a boundary between discrete grains. Once the boundary has high-angle character, its mobility increases by up to several orders of magnitude (Humphreys and Hatherly, 2004, p. 127), and grain-boundary migration will modify the shape and possibly the size of the new grains. As a result, the new grains become microstructurally distinct, as well as having significantly different orientations to the host grains. The SGR mechanism suggests that the new grains initially have the same size as the subgrains from which they are derived. Based on a model assuming grain growth driven by strain energy, Shimizu (1998) proposed a temperature-dependent grainsize-stress relationship with an exponent between 1.25 and 1.33. The controls over sub-grainsize, and the evolution of the grainsize once the new grains have formed, are discussed further below.

2.3. Recrystallization by unrestricted grain-boundary migration

Experimental work on a variety of materials suggests that at relatively high temperatures and low stresses, grain-boundary migration becomes pervasive, producing a microstructure that is quite distinct from that associated with the BLG and SGR nucleation mechanisms (Hirth and Tullis, 1992). This is supported by observations on naturally deformed rocks (Dunlap et al., 1997; Jessell, 1987; Stipp et al., 2002b). Grains may have straight or broadly

lobate boundaries, giving them an amoeboid shape, and there may be evidence for exaggerated growth of individual grains. This mechanism has been referred to as "migration recrystallization" or GBM, but these terms could cause confusion, as BLG also involves migration of grain boundaries. For this reason we use GBR.

GBR sweeps out dislocations and produces new lattice, but does not necessarily involve nucleation. Hirth and Tullis (1992) cite evidence for nucleation by SGR under Regime 3 conditions, but unrestricted grain-boundary migration will tend to eliminate the microstructural evidence for nucleation processes (Stipp et al., 2002a). Many of the current theories to explain grainsize-stress relationships have been developed assuming nucleation by BLG or SGR, followed by relatively rapid grain-boundary migration driven either by strain energy (Derby, 1992) or surface energy (Austin and Evans, 2007). The controls on these processes are discussed in more detail below.

3. Grainsize evolution during dynamic recrystallization

3.1. Controls on nucleation size

The main control on the size of new grains formed by the BLG mechanism is likely to be the length scale of variations in dislocation density in the grains on either side of the boundary. Even in weakly recovered materials, dislocations tend to be loosely organized into cell structures (Humphreys and Hatherly, 2004), and these define the scale of dislocation density variation. There is some observational evidence that grain-boundary bulging is controlled by the presence of sub-grain or cell walls in the grain being invaded (Hirth and Tullis, 1992), and grain-boundary migration during high temperature creep may be controlled by the scale of sub-grain structures on both sides of the boundary (Derby, 1991; Humphreys and Hatherly, 2004). As noted above, surface energy considerations dictate that at any given stress there is a lower limit to the size of the bulges that can form (the $D_{\min}$ line, Eq. (6)), but the slope of this line does not correspond to the experimentally observed grainsize-stress relationship. We therefore suggest that the size of many of the the nuclei formed by BLG is controlled by cell size or sub-grainsize. The grainsize distribution is likely to extend to smaller sizes than the sub-grainsize, however, as some bulges may be related to dislocation density variations at a smaller scale.

The SGR mechanism also requires that the new grains have the same initial size as the subgrains from which they are derived (Shimizu, 1998). Subgrains tend to be smaller near grain boundaries, however, so the new grains may be somewhat smaller than the mean size of subgrains within deformed older grains.

It seems likely, therefore, that nuclei formed by both the SGR and BLG mechanisms are broadly related to the size of subgrains, and where both nucleation mechanisms are operative, the new grains are commonly about the same size (e.g., Stipp and Kunze, 2008, and see also below). The size of both transient dislocation cells and subgrains is generally considered to be inversely related to stress with an exponent q of around 1 (De Bresser et al., 2001; Humphreys and Hatherly, 2004; Poirier, 1985). If the size of nuclei produced by the BLG and SGR mechanisms is controlled by these structures, this could provide an approximate explanation for the empirically observed recrystallized grainsize-stress relationship. We therefore explore models for sub-grainsize in more depth.

3.2. Controls on sub-grainsize

The diameter of both transient dislocations cells and subgrains is likely to decrease with increasing dislocation density, to allow greater numbers of dislocations to be accommodated within the arrays that define the cell or sub-grain walls. In general, the majority of dislocations are fated either to leave the crystal entirely, or to annihilate with a dislocation of the opposite sign. The dislocations that end up being incorporated in sub-grain walls are therefore largely *geometrically necessary* dislocations: those that are required to produce the permanent and visible distortion of the crystal lattice, resulting from the boundary conditions imposed by adjacent grains. The relationship between the sub-grainsize and the flow stress may therefore be indirect. Nevertheless it is widely accepted that sub-grain diameter d_s is related to the flow stress by:

$$\frac{d_s}{b} = K_s\left(\frac{\sigma}{\mu}\right)^{-q} \tag{7}$$

where μ is the shear modulus, b is the Burgers vector (the lattice offset associated with an individual dislocation), K_s is a material constant, and the exponent q is approximately one (Poirier, 1985; Twiss, 1977; Shimizu, 2008).

Humphreys and Hatherly (2004) suggest three alternative mechanisms that could lead to a relationship between sub-grain diameter and stress.

a) The sub-grainsize limits the mean free path for dislocation glide, decreasing the strain rate achievable at a given dislocation density ρ, and therefore increasing the value of ρ, and hence σ, required for a given imposed strain rate. This is the Hall-Petch effect, and predicts $q = 2$.
b) The dislocation density is controlled by the activity of dislocation sources (such as Frank-Read sources) that have a scale-length related to d_s. This predicts $q = 1$.
c) The dislocations housed in the sub-grain walls can be averaged over the microstructure to calculate ρ, and hence σ. This gives $\rho = C_1/(d_s h)$, where h is the spacing of dislocations in the sub-grain walls and C_1 is a geometrical constant related to the shape of the subgrains. For constant h, this predicts $q = 2$.

None of these explanations is entirely satisfactory, and (a) and (c) do not predict the observed relationship. Mechanism (a) implies that the formation of subgrains results in hardening, whereas in fact it is accompanied by a reduction of dislocation density and hence softening. Mechanism (b) is more likely to apply to the small, transient, low-misorientation dislocation cells that form during deformation, rather than to the larger, quasi-permanent structures that we see as optically visible subgrains. Mechanism (c) would only apply if static recovery had completely eliminated all the dislocations within the subgrains. During dynamic recovery, however, unbound dislocations (i.e., those not housed in sub-grain walls) are continuously being generated, and are required to produce ongoing crystal-plastic deformation (Humphreys and Hatherly, 2004).

A possible explanation for the experimentally observed relationship between sub-grainsize and stress during dynamic recovery arises from the following two propositions. First, during dynamic recovery of a single-phase polycrystalline aggregate, the proportion of geometrically necessary dislocations to unbound dislocations may be approximately constant. The second proposition is that the spacing of dislocations in the sub-grain walls is inversely proportional to stress, as is implied by the increase in energy density of a sub-grain wall with misorientation (Humphreys and Hatherly, 2004). If the size of the subgrains decreases until their walls can accommodate all the geometrically necessary dislocations, $q = 1$ (see also Shimizu, 2008). The linear relationship between stress and misorientation suggests that the SGR mechanism will produce new grains most rapidly in areas of stress concentration, such as along

grain boundaries, and this provides an explanation for the development of core and mantle structure (White, 1976), in which new grains are preferentially developed around the margins of old grains.

There are very few studies in the geological literature concerning the relationship between sub-grainsize and stress in rock-forming minerals, or between sub-grainsize and recrystallized grainsize. Twiss (1977) calibrated the relationship between subgrain diameter and flow stress using experimental data on metals and minerals, to obtain a value for q of 1 ± 1.03. Ross et al. (1980) obtained 0.62 and 0.69 in experiments on dry and wet olivine respectively. Schmid et al. (1980), in experiments on calcite, noted that the sizes of subgrains and recrystallized grains were identical, with an exponent in the relationship to stress of 1.01 ± 0.05. De Bresser et al. (2001) summarize an extensive database on subgrainsize and recrystallized grainsize in a variety of crystalline materials. The data show substantial scatter, but generally support a somewhat lower exponent for the subgrain-size *vs* stress relationship than for the recrystallized grainsize-stress relationship. We therefore need to examine the extent to which grainsize changes after nucleation.

3.3. Grainsize evolution after nucleation

The process of nucleation by the BLG mechanism involves an initial stage of growth of the bulge, driven by the strain energy difference between the bulge and the surrounding work-hardened material. Surface energy will resist growth, because growth increases surface area, but if the bulge is able to reach a radius of D_{min} (see Eq. (2)) the effect of surface energy will be smaller than the strain energy term. As the new grain grows it will be deformed, and the dislocation density will increase (Fig. 1b), reducing the driving force for further growth (Derby and Ashby, 1987; Humphreys and Hatherly, 2004). Once new grains start to impinge on each other and form a recrystallized aggregate, their boundaries may migrate in either direction depending on the dislocation density difference across the boundary. As the dislocation density in a grain increases with deformation, there is an increasing probability that it will start to be consumed by neighboring grains. The new grains will end up with dislocation densities that fluctuate about a mean, and their boundaries will be in continuous more-or-less random motion, driven by the local differences in dislocation density across them (Fig. 2). This migration is part of the process of dynamic recrystallization: it may not produce new grains as such, but it produces new dislocation-free lattice behind the migrating boundaries.

The most widely cited concept to explain the empirical grainsize-stress relationship involves an equilibrium between grainsize reduction (by nucleation processes) and grain growth. Theories to explain this "equilibrium" grainsize invoke either strain energy or surface energy as the driving force for grain growth. Derby and Ashby (1987), for example, proposed that a mean grainsize is established as a result of a balance between the rate of nucleation of grains by the BLG mechanism and the rate of subsequent growth driven by the strain energy associated with dislocations in subgrain walls. They developed a statistical theory for the rate of nucleation, and predicted a recrystallized grainsize-stress relationship with an exponent p between 1.4 and 2.5. Derby (1991) supported this concept with an empirical grainsize-stress plot suggesting $p = 1.5$. Derby (1992), however, states that there was an error in the theory, and that the predicted value for p should be 3. Shimizu (1998), (2008) advanced a similar model invoking nucleation by sub-grain rotation, with subsequent growth driven by the strain energy associated with both free dislocations and dislocations stored in sub-grain walls, and predicted values for p between 1.25 and 1.33. De Bresser et al. (1998) proposed that grainsize reduction by dynamic recrystallization might result in an increase in the rate of grainsize-sensitive creep, and a decrease in the rate of dislocation creep. The grainsize would then increase until the strain rates accommodated by dislocation creep and by grainsize-sensitive creep were the same. They therefore propose that the piezometric relationship between stress and D_r should lie on the field boundary between two deformation mechanisms. Austin and Evans (2007) proposed that D_r reflects the rate of energy dissipation produced by creating new grain-boundary area by dynamic recrystallization and reducing grain-boundary area per unit volume by surface energy driven grain growth.

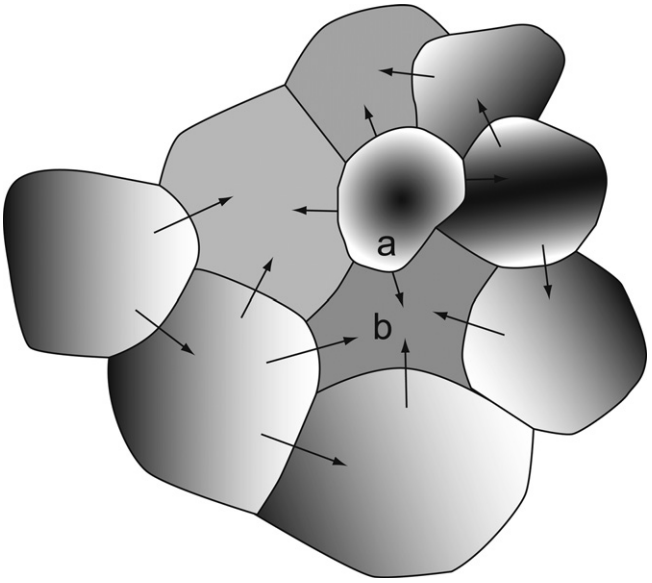

Fig. 2. Strain energy driven GBM (ρGBM) in a recrystallized aggregate. Grain boundaries migrate in the direction of greater dislocation density (darker shading), and leave low-density dislocation lattice behind them. Although some grains are growing and some are shrinking, others have boundaries migrating both inwards and outwards. The overall net migration direction in a large aggregate is random. Growing grains (for example grain *a*) have boundaries that are convex outward, because the boundaries are bulging into neighboring grains and pinned at the vertices; shrinking grains (for example grain *b*) have boundaries that are concave outward. This is the opposite pattern of curvature to that produced by surface energy driven GBM (γGBM, compare Fig. 3). ρGBM therefore tends to oppose γGBM.

In view of the above discussion it is worth examining in some detail the driving forces for grain growth during dynamic recrystallization. As noted above, in a recrystallized aggregate where the dislocation density fluctuates about a mean, grain-boundary migration driven by strain energy (henceforth ρGBM) will be essentially random. As shown in Fig. 2, there is nothing about the topology of the aggregate that predicts a net change in grainsize: different boundaries of the same grain may migrate either toward or away from the grain center, and because larger grains tend to be consumed by smaller grains, which grow in the process, the net effect is a reduction in variance rather than a change in the mean. Grain *growth* driven by strain energy will therefore cease once the material is fully recrystallized, even while ρGBM continues to maintain the steady state microstructure.

The surface energy term, on the other hand, does provide a driving force for growth in the recrystallized aggregate, as an increase in the average grainsize reduces the surface area per unit volume of the aggregate. The rate of grain-boundary migration v depends on the driving force and the mobility M. For grain-boundary migration driven by surface energy (henceforth γGBM), the driving force is related to the surface energy per unit area γ and

the radius of curvature R_b of the boundary (Humphreys and Hatherly, 2004; Eq. 11.2), so the boundary migration velocity is:

$$v_r = 2M\gamma/R_b \tag{8}$$

The direct effect of the surface energy term is to reduce the curvature of grain boundaries, and to adjust the interfacial angles around triple junctions to 120° by migration of the vertices. As shown in Fig. 3, in an aggregate of grains with similar grainsizes, the smaller grains tend to have fewer faces, and for topological reasons this means that the faces tend to be convex outward (Humphreys and Hatherly, 2004). The surface energy term tends to straighten out these faces, and hence reduce the size of the smaller grains, which tend to disappear. Conversely, grains larger than the average tend to have faces with convex-inward curvature, and the surface energy term causes these grains to grow. The net effect is an increase in average grainsize.

For ρGBM, the grain-boundary migration velocity is:

$$v_\rho = ME_d \tag{9}$$

The ratio of the velocities produced by γGBM and ρGBM is $v_\gamma/v_\rho = 2\gamma/R_bE_d$, and hence from Eq. (5),

$$\frac{v_\gamma}{v_\rho} = \frac{8\pi\mu\alpha^2\gamma}{R_b\chi\sigma^2\ln(\alpha\mu\beta/2\sigma)} \tag{10}$$

If we assume that R_b is proportional to grainsize (Burke and Turnbull, 1952), then this ratio will decrease with increasing grainsize. When the grainsize is close to the critical size for grain-boundary bulging (D_{min}, see Eq. (6)), R_b is likely to be close to the grain radius. Comparison between (6) and (10) shows that the velocity ratio will therefore be close to unity when the grainsize equals D_{min}. For any grainsize greater than D_{min}, the migration velocity produced by dislocation strain energy will on average be larger than that produced by surface energy. The first-order topology of the grain boundaries will therefore be primarily controlled by ρGBM.

There is a further important implication arising from the fact that γGBM acts to reduce the curvature of grain boundaries, which means that the direction of γGBM is always toward the center of curvature (Fig. 3). This is in the opposite direction to that produced by strain energy driven ρGBM, which drives motion away from the center of curvature (Fig. 2). Hence the two processes are antagonistic, and whichever mechanism produces the highest rate of GBM will dominate the microstructure. Under conditions for which strain energy results in a higher rate of GBM, γGBM will be confined to reducing small-scale curvature and limiting the formation of bulges with sizes less than D_{min}. Neither of these processes are likely to lead to grain growth. Below the D_{min} line, γGBM will dominate, and will lead to grain growth following the normal grain growth law (Humphreys and Hatherly, 2004). Some examples of microstructures involving BLG and SGR recrystallization mechanisms accompanied by ρGBM are shown in Figs. 4 and 5.

The conclusion of this section is that neither dislocation strain energy nor surface energy provide an effective mechanism for grain

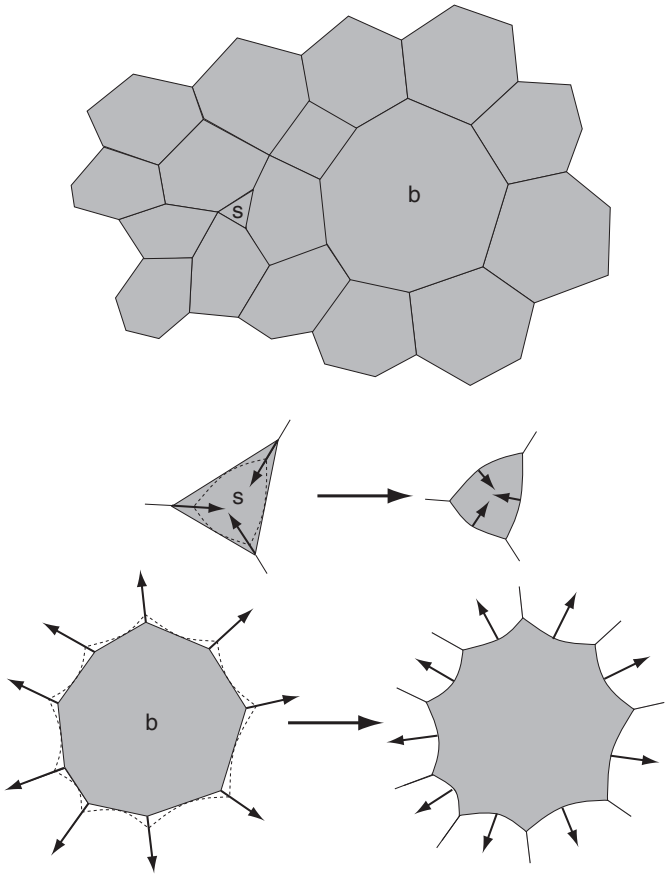

Fig. 3. Surface energy driven GBM (γGBM) in a recrystallized aggregate. Vertices migrate as shown in the lower two left–hand diagrams to equalize angles at 120° (in 2-D). This causes the faces to become curved, and these in turn migrate to reduce the curvature (lower two right hand diagrams). As a result, small grains (s) tend to shrink and eventually disappear, and big grains (b) tend to grow, resulting in an increase in the average grainsize. Growing grains have boundaries that are concave outward, and shrinking grains have boundaries that are convex outward. This is the opposite pattern of curvature to that produced by ρGBM (compare Fig. 2).

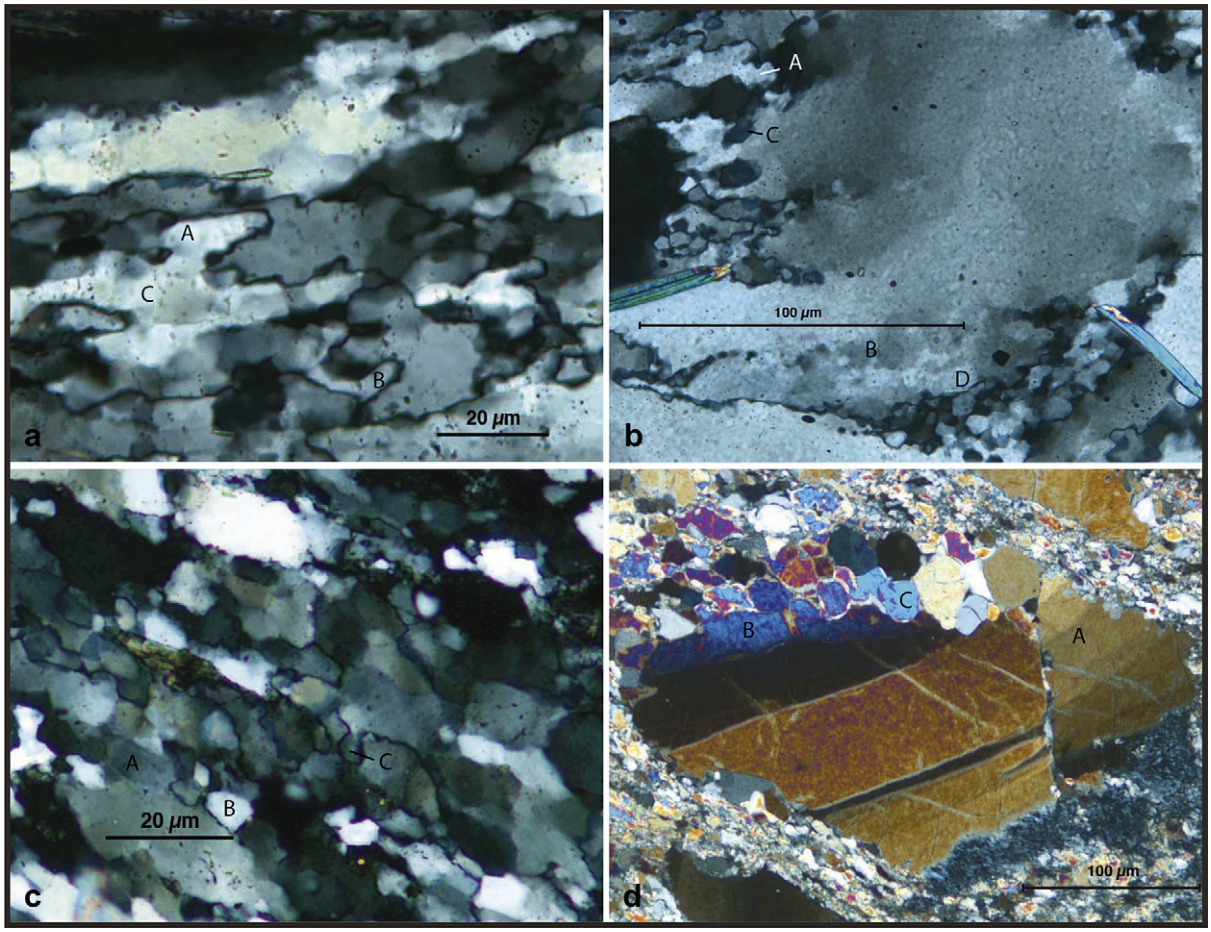

Fig. 4. Optical micrographs. All sections are normal to foliation, parallel to lineation. a) Bulges produced by ρGBM in quartz (A), together with new grains created by the BLG mechanism (B). Bulges and new grains are similar in size. Subgrains are also visible within the deformed grains (C). Foliation is horizontal in the image. Pt493, mylonitic quartzite, Sierra Alhamilla, Spain. b) Quartz porphyroclast invaded by bulges along the margin (A), and with internal sub-grain structure (B). New grains produced by the BLG (C) and SGR (D) mechanisms at the expense of an earlier population of large annealed quartz grains are all of similar size to each other and to the bulges and subgrains. Foliation is horizontal in the image. CN19, metachert, Santa Catalina Island, California. c) Subgrain structure in deformed quartz (A) showing transition to new grains of similar size (B). The subgrains have fairly planar boundaries, but the new grains show evidence of modification of their shapes by ρGBM. There is also evidence for nucleation by bulging (C). Foliation is gently inclined to the right. Pt481, mylonitic quartzite, Sierra Alhamilla, Spain. d) Olivine porphyroclast showing subgrains (A), progressive sub-grain rotation to form new grains (B), and modification of the shapes of the new grains by ρGBM (C). The new grains are comparable in size to the subgrains. Foliation is gently inclined to the right. Mylonitic peridotite, Finero massif, southern Alps.

growth in a dynamically recrystallized aggregate lying above the D_{min} line in grainsize-stress space, although the grain boundaries may be migrating vigorously under the effects of strain energy. We emphasize that this conclusion is original to this paper, and is contrary to currently accepted ideas. We invite the reader to carefully compare the patterns of grain-boundary migration for ρGBM and γGBM in Figs. 2 and 3. The grain-boundary topology and directions of grain-boundary migration are fundamentally different. γGBM leads directly to the shrinkage of small grains and the growth of large grains; ρGBM does not.

Our conclusion that ρGBM does not lead to grain growth in a recrystallized aggregate limits the application of concepts that depend on grain growth acting in competition with grainsize reduction by dynamic recrystallization. The mechanisms for reaching an equilibrium grainsize proposed by Derby and Ashby (1987) and Shimizu (1998), (2008), which depend on the growth of new grains by ρGBM at the expense of old, pre-existing grains, can only operate during the initial stages of dynamic recrystallization. Once continuous volumes of recrystallized material have formed, these concepts no longer apply. The field boundary concept proposed by De Bresser et al. (1998), and the paleowattmeter concept of Austin and Evans (2007), are therefore limited to the γGBM field, below the D_{min} line.

In view of the restriction on grain growth above the D_{min} line, we suggest that D_r is controlled primarily by nucleation processes in the ρGBM field. It is therefore of some importance to determine the position of the D_{min} line in stress-grainsize space as precisely as possible. The slope of the line is well defined by Eq. (6), but its position is sensitive to both the strain energy term E_d and the surface energy term γ, neither of which are very well constrained. Measured values for quartz interfacial energy in wet environments vary from 0.27 ± 0.11 Jm^{-2} (Hiraga et al., 2007) to 0.385 Jm^{-2} (Parks, 1984), and much higher values have been determined for quartz in air and in vacuum (Parks, 1984; and references therein). If we use a value of 0.27 Jm^{-2} in Eq. (6), and calculate E_d from Eq. (5) using parameter values listed in Table 1, the D_{min} line intersects the piezometric line for quartz at 9 μm (dashed purple line in Fig. 6). Microstructural observations, however, suggest that BLG and ρGBM proceed at significantly larger grainsizes than this, however (see below for further discussion). Our preferred position for the D_{min} line is shown in solid purple in Fig. 6. This corresponds to a value for γ of 0.1 Jm^{-2}, which is well below the range of experimental values.

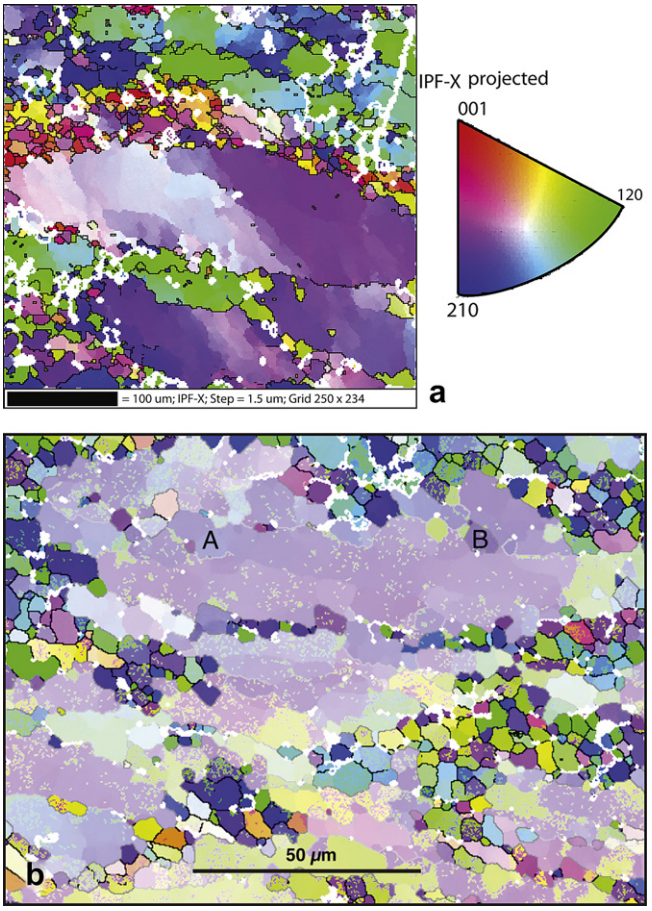

Fig. 5. Electron backscatter diffraction images (EBSD). Colors indicate grain orientations relative to the *X*-direction (horizontal), keyed to the inverse pole figure (top right). Sections are normal to foliation, parallel to lineation (horizontal in figures). a) Quartz porphyroclast with internal sub-grain structure, and extensive invasion of the grain-boundary by bulging. Many of the recrystallized grains around the margin have formed by the BLG mechanism, and the new grains are similar in size to the bulges. Recrystallized grains have shapes suggesting modification by ρGBM, but there is no evidence for grain growth. Pt490, mylonitic quartzite, Sierra Alhamilla, Spain. b) Deformed quartz porphyroclasts surrounded by dynamically recrystallized matrix. Porphyroclasts show internal sub-grain structure (A), and evidence for recrystallization by SGR (B). Much of the recrystallized matrix may have formed by SGR, but the grain shapes have clearly been modified by ρGBM, and there is no evidence for grain growth. PW79, mylonitic quartz vein in granitoid, Whipple Mtns, SE California.

It may reflect the actual value of the surface energy for quartz in a metamorphic environment, or it may be a result of uncertainties in the other parameters in Eq. (5). Our preferred position places the intersection of the D_{min} and piezometry curves for quartz at about 70 μm grainsize. Note that both the D_{min} line and the piezometry line are independent of temperature, as is the intersection.

The interfacial energy of olivine is also rather poorly known; in Fig. 7 we use a value of 1.4 Jm^{-2} determined from microstructural observations by Duyster and Stockhert (2001). With this value the intersection of the D_{min} and piezometry curves for olivine is at 35 μm. The position of this intersection for both minerals is highly uncertain at present, however, and will change as more accurate data on surface energies and piezometric relationships become available.

4. Implications of grainsize evolution for paleopiezometry

BLG nucleation can only take place above the D_{min} line, and as discussed above, new grains formed by the BLG mechanism will not grow once they form part of a recrystallized aggregate. This is consistent with observational evidence from rock-forming minerals that have recrystallized by BLG, in which the recrystallized grainsize is commonly similar to the size of grain-boundary bulges (Figs. 4a, b, and 5a). SGR nucleation is possible below the D_{min} line, but the coexistence of the BLG and SGR mechanisms in some rocks (Fig. 4b) suggests that it may also occur above the line. The restriction on grain growth therefore applies to at least some rocks in which the dominant recrystallization mechanism is SGR, and this is supported by the fact that new grains formed by SGR are commonly the same size, or somewhat smaller, than subgrains in the same rock (Figs. 4c, d and 5b). We propose above that nuclei formed by the BLG and SGR mechanisms are both controlled by dislocation cell or sub-grainsize, and that there is no grain growth in the recrystallized aggregate for materials deformed above the

Table 1
Parameters and values. References: 1, Twiss (1977); 2, Karato and Wu (1993); 3, this paper; 4, Devincre et al. (2008); 5, Stipp and Tullis (2003), Holyoke and Kronenberg, (2010); 6, van der Wal et al. (1993); 7, Berman (1988); 8, Holland and Powell (1998); 9, Shimizu (2008); 10, Brady (1994); 11, Dolmen et al. (2002); 12, Hirth et al. (2001); 13, Farver and Yund (2000a); 14, Farver and Yund (2000b).

Parameter	Explanation	Quartz	Olivine	Reference
b	Burgers vector (m)	5.00E-10	5.00E-10	1, 2
C_2	constant in Eqs. (11) and (12)	3	3	3
D_r	dynamically recrystallized grainsize (m)			
d_s	sub-grainsize (m)			
E_d	dislocation strain energy/volume (Jm^{-3})			
g	constant in Eq. (13)	7.5	7.5	4
k	Boltzmann's constant (JK^{-1})	1.38E-23	1.38E-23	
K	piezometric constant (μm MPa^p)	2451	1.50E+04	5, 6
L	dislocation mean free path length (m)			
p	grainsize exponent	1.26	1.33	5, 6
q	subgrain-size exponent			
n	exponent in power-law eqn			
R	gas constant (JK^{-1} mol^{-1})	8.314	8.314	
R_b	grain-boundary curvature (m)			
r	radius of a grain-boundary bulge (m)			
T	temperature (K)			
V	molar volume (m^3 mol^{-1})	2.37E-05	4.37E-05	7, 8
v_g	dislocation glide velocity ($msec^{-1}$)			
v_γ	rate of γGBM ($msec^{-1}$)			
v_ρ	rate of ρGBM ($msec^{-1}$)			
$\dot{e}$	strain rate (sec^{-1})			
α	constant in Eq. (4) [a]	1	1	
χ	constant in Eq. (3)	1.18	1.33	9
β	constant in Eq. (3)	3.00	3.00	9
γ	surface energy (Jm^{-2})			
μ	shear modulus (Pa)	4.20E+10	8.00E+10	1, 2
ρ	dislocation density (m^{-2})			
σ	differential stress (Pa)			
D_{0v}	coefficient for volume diffusion (m^2sec^{-1})	2.00E-10	6.31E-05	10, 11
Q_v	activation energy for self diffusion (J mol^{-1})	145000[b]	529000	12, 11
wD_{0gb}	grain-boundary width × coefficient for grain-boundary diffusion (m^3sec^{-1})	2.54E-16	1.39E-14	13
Q_{gb}	activation energy for grain-boundary diffusion (J mol^{-1})	137000	375000	14
$f(H_2O)$	water fugacity (MPa)			
F(dis)	scaling factor for dislocation creep	7.00-8	1.00-5	[c]
F(DRX)	scaling factor for DRX creep	4.00-7	1.00-7	[c]
F(diff)	scaling factor for diffusion creep	4.00-7	5.00E-03	[c]

[a] Kohlstedt and Weathers (1980) give $\alpha = 3$, but their experimental data are not consistent with Eq. (4), which invalidates this value.
[b] Q_v for quartz was adjusted from experimentally determined values as discussed in the Appendix.
[c] See Appendix for discussion of the scaling factors.

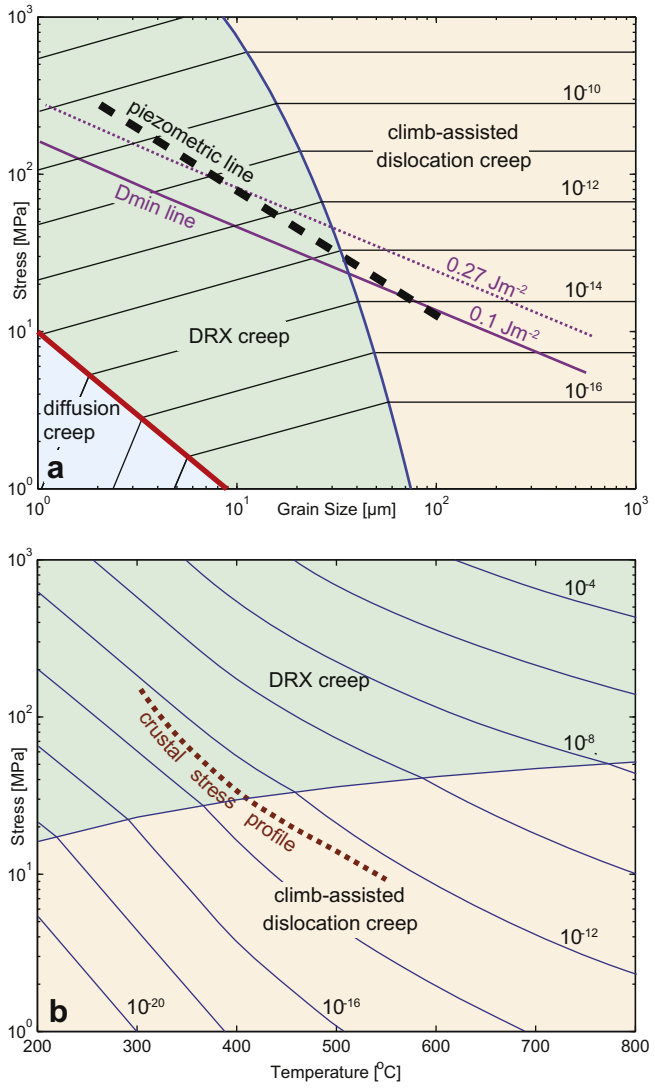

Fig. 6. a) Stress-grainsize map for quartz at 400 °C. Deformation mechanism fields are shown for theoretical climb-assisted dislocation creep, DRX creep (see text), and diffusion creep (see Appendix for flow laws and parameter values). Strain rates and field boundaries are illustrative only, but the topology is robust. The piezometric line is after Stipp and Tullis (2003), corrected after Holyoke and Kronenberg (2010). The D_{min} line (solid purple) is calculated from (6) for $\gamma = 0.1$ Jm^{-2}, the dotted purple line is for $\gamma = 0.27$ Jm^{-2}. Above the D_{min} line ρGBM is dominant, and grain growth by γGBM will be inhibited; below the D_{min} line γGBM is dominant, and recrystallized grainsize may be modified by grain growth. b) Stress-temperature map constructed assuming that the grainsize follows the piezometric relation shown in (a). The field boundary is the locus in stress-T space of the intersection of the DRX/dislocation-creep boundary with the piezometric line in (a). Crustal stress-T profile from Behr and Platt (2011).

D_{min} line. This implies firstly that D_r is controlled primarily by nucleation processes under these conditions, and hence by the subgrain or cell size. This concept provides a first-order explanation of the approximately inverse linear grainsize-stress relationship that is observed experimentally, although it does not explain the precise value of the stress exponent determined by Stipp and Tullis (2003).

If nucleation occurs by the SGR mechanism below the D_{min} line, γGBM will be dominant, and the mean size of the recrystallized aggregate will increase (note that the formation of new grains by SGR will not be inhibited by surface energy considerations, because they evolve from subgrains that have much lower surface energy). Grain growth in the recrystallized aggregate should in principle proceed until the grains reach the D_{min} line (Fig. 7). As a result, the grainsize-stress relation may depart from the projection of the empirical curve and approach the D_{min} line. This has not been experimentally observed, but we suggest this happens below the lower stress limit of the experimental data. If it does happen, it opens up the possibility that below the D_{min} line, a new generation of grains may form by SGR within the enlarged grains formed in an earlier stage of recrystallization, and the resulting average grainsize may reflect the competition between these competing processes, as suggested by De Bresser et al. (1998) and Austin and Evans (2007).

5. Implications of grainsize evolution for recrystallization regimes

The relationships described above provide a basis for interpreting the microstructural regimes recognized in deformed quartz by Hirth and Tullis (1992), and subsequently modified for natural rocks by Stipp et al. (2002a), (2002b), (2010). *Regime 1* corresponds to the high stress state in which grains only nucleate by BLG. We would argue that this must lie above the D_{min} line, at very high stresses and hence small grainsizes, and in the DRX creep field (Fig. 6). *Regime 2* corresponds to that part of the field of SGR nucleation that lies above the D_{min} line. Nucleation by BLG is also possible, as suggested by Stipp et al. (2002a); the sizes of new grains formed by both mechanisms will be controlled by the prevailing sub-grainsize, and follow the empirical grainsize-stress relationship. *Regime 3* is less easy to interpret. The experimental microstructure described as Regime 3 by Hirth and Tullis (1992) has a grainsize of <10 μm (Stipp and Tullis, 2003), and shows evidence of extensive ρGBM: this is likely to have formed above the D_{min} line, and may correspond to complete recrystallization in the ρGBM field. We suggest that the relatively coarse-grained microstructure described in natural rocks by Stipp et al. (2002a), (2002b), (2010) as GBM (corresponding to our GBR mechanism), however, forms in the area of stress-grainsize space below the D_{min} line. Nucleation by BLG is not possible in this field; grains may nucleate by SGR, and then grow by γGBM. The clear evidence for grain growth in rocks showing this microstructure suggests that grain-boundary migration is surface energy driven. If, as suggested above, the grainsize in the γGBM field tends to evolve toward the D_{min} line, the microstructure may show the effect of both processes of grain-boundary migration, leading to the poorly defined grainsize distribution and irregular grain shapes commonly observed in this field.

If this interpretation is correct, it implies that the intersection between the D_{min} line and the piezometer corresponds to the SGR/GBR boundary. Stipp et al. (2010) suggest that in nature this occurs at a dynamically recrystallized grainsize of ~120 μm. This therefore places an observational constraint on the position of this intersection, and hence on the value of the surface energy of quartz, which controls it. It is for this reason we chose the position of the D_{min} line for quartz shown in Fig. 6.

6. Strain-induced GBM as a recovery mechanism: rheological implications

Strain-induced GBM in a dynamically recrystallized aggregate acts to reduce the mean dislocation density; hence it counteracts work-hardening, and is analogous in its effects to intracrystalline recovery processes. At high strain rates and low temperatures, climb-assisted recovery may not be fast enough to keep pace with work-hardening, whereas ρGBM effectively sweeps out high dislocation density lattice and replaces it with new lattice with low dislocation density. The newly recrystallized material is relatively weak, hence it deforms, and the dislocation density in it builds up again. At steady state, the mean dislocation density in the aggregate therefore reflects a balance between the rate of destruction of

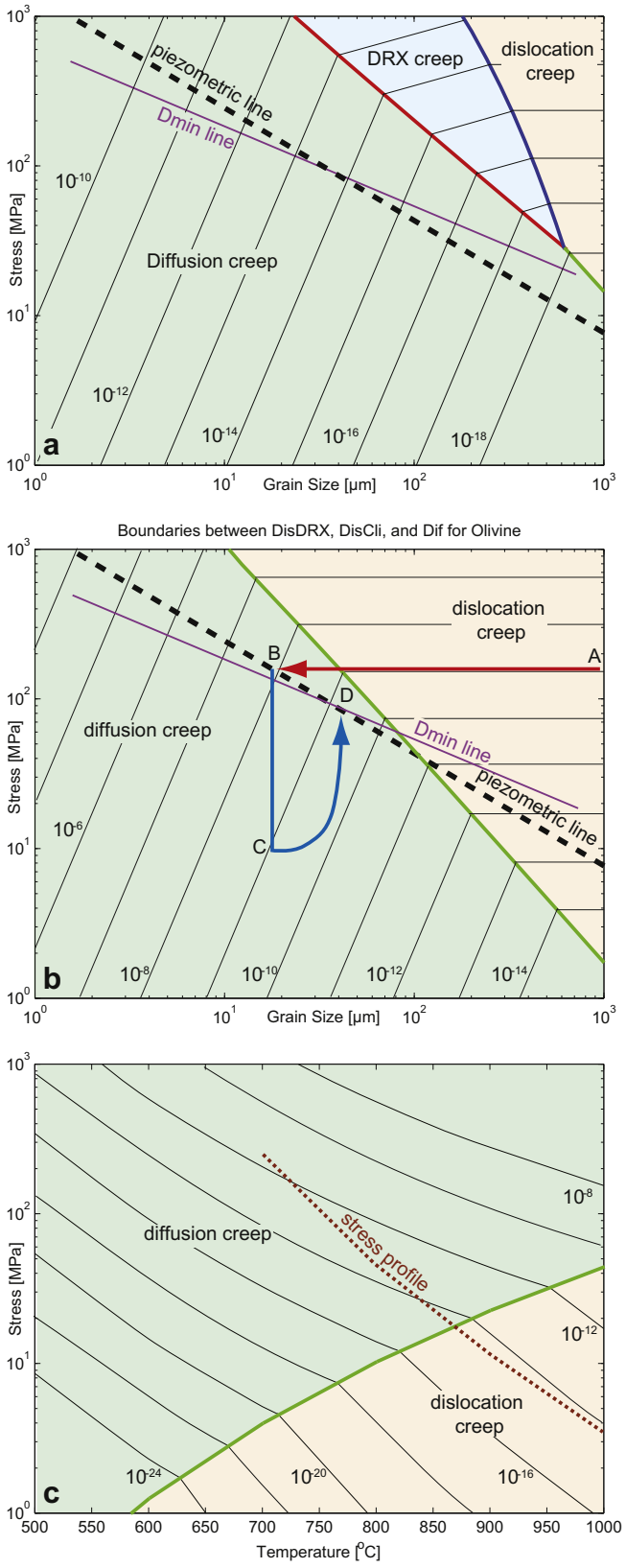

Fig. 7. a) Stress-grainsize map for olivine at 700 °C. The piezometric line is after van der Wal et al. (1993). The D_{min} line is calculated from Eq. (6) using a surface energy of 1.4 Jm^{-2}. b) Stress-grainsize map for olivine at 1000 °C. The grainsize evolution is shown for a peridotite with an initial grainsize of 1 mm, deformed at 170 MPa differential stress (point A). Dynamic recrystallization reduces the grainsize to 18 μm, on the piezometer line (point B). If the rock is in a shear zone deforming at constant stress, there is no further grainsize evolution, because the rock is above the D_{min} line. If the rock deforms at constant strain-rate, the stress will drop to 10 MPa (point C), at which point the rock lies below the D_{min} line. Grain growth may therefore occur, and the rock may evolve back to toward the field boundary (point D), as suggested by De Bresser et al. (2001). c) Stress-temperature map constructed assuming that the grainsize follows the piezometric relation. A possible stress-T profile through the lithospheric mantle is shown to illustrate how the dominant deformation mechanism may change with depth.

dislocations by the migrating boundaries, and the average rate of dislocation multiplication in the aggregate. The rate of elimination of dislocations $\dot{\rho}_R$ by grain-boundary migration at velocity v_ρ will depend on the surface area/volume ratio of the recrystallized grains, so

$$\dot{\rho}_R = C_2 \rho v_\rho / D_r \tag{11}$$

where C_2 is a geometrical constant ~3.

If dislocation multiplication is primarily due to Frank-Read sources, they will consist mainly of expanding loops with an average radius equal to the mean free path length L for dislocation glide. If there are m loops/volume, the rate in increase of dislocation line length per unit strain is

$$\left(\frac{d\rho}{de}\right)_H = \frac{2\pi L m}{\rho b L} = \frac{1}{bL} \tag{12}$$

(see also Poirier, 1985, Eq. (4.19). But at steady state, the Bailey–Orowan relationship can be expressed as

$$\dot{e} = \left(\frac{d\rho}{dt}\right)_R \Big/ \left(\frac{d\rho}{de}\right)_H \tag{13}$$

(see Poirier, 1985, p. 108), and hence,

$$\dot{e} = \frac{C_2 \rho v_\rho b L}{D_r} \tag{14}$$

This is a form of Orowan's transport equation, in which the rate-controlling velocity is the grain-boundary migration velocity.

From Eqs. (5), (9), and (4),

$$\dot{e} = \frac{C_2 L M \sigma^4 \chi \ln(\alpha\mu\beta/2\sigma)}{4\pi\alpha^4\mu^3 b D_r} \tag{15}$$

M is the grain-boundary mobility, which is likely to be strongly affected by the composition of fluid phases and impurities along the boundaries. It probably has the form $M = M_0 \exp(-Q_{gb}/RT)$, where Q_{gb} is the activation energy for grain-boundary diffusion.

Eq. (15) predicts a new form of grainsize-sensitive dislocation creep, which we refer to as the DRX controlled dislocation creep flow law to distinguish it from conventional climb-controlled dislocation creep flow laws. It can be compared with the theoretical flow law for climb-controlled dislocation creep (see Appendix); this has a stress exponent of three, which results from the stress-dependence of both the dislocation density (4) and the rate of climb (Poirier, 1985). DRX creep has a stress exponent of four, because both the strain rate and the rate of grain-boundary migration depend on the dislocation density.

Grainsize sensitivity within the dislocation creep field, particularly near the boundary with diffusion creep, has been recognized experimentally by Hirth and Kohlstedt (2003), who attribute it to a component of dislocation creep-accommodated grain-boundary sliding. Although there is evidence for grain-boundary sliding under these conditions, we suggest that for rocks deforming by the BLG mechanism, the recrystallization flow law we propose will dominate the strain rate just as it dominates the microstructure.

The two grainsize-sensitive dislocation creep regimes can be distinguished by their different grainsize exponents: dislocation creep-accommodated grain-boundary sliding should have an exponent of −2, whereas DRX controlled dislocation creep has an exponent of −1. They may also be distinguishable by the relative strength of lattice preferred orientations in the material—DRX controlled dislocation creep will maintain a strong crystallographic preferred orientation, whereas grain-boundary sliding will weaken it significantly (Precigout et al., 2007; Warren and Hirth, 2006).

Calculation of strain rates using this theoretically derived flow law is limited by uncertainties in some of the parameters. Experimental estimates of the grain-boundary mobility M for olivine by Evans et al. (2001) vary by three orders of magnitude even at constant temperature, for example, and it is likely to be strongly influenced by the presence and composition of a fluid phase. The value of L, the mean free path for dislocations, is also uncertain. This is central to the concept of strain-hardening, which Devincre et al. (2008) describe as a "long-standing challenge to dislocation theory". On the basis of numerical modeling of dislocation interactions, they suggest that it has the form $L = g\mu b/\sigma$, with g dependent on crystal orientation. For FCC metals, g is in the range 4.6–10.4. This then gives:

$$\dot{e} = \frac{C_2 g M \sigma^3 \chi \ln(\alpha\mu\beta/2\sigma)}{4\pi\alpha^4\mu^2 D_r} \tag{16}$$

If we assume that the grainsize is controlled by dynamic recrystallization, and follows the empirical grainsize-stress relationship, the effective stress exponent is increased by p. The flow law then has an effective stress exponent of $3 + p$, which is slightly over 4. This corresponds well with the suggestion by Hirth et al. (2001) that the stress exponent in natural quartz mylonites is about 4.

7. Deformation mechanism maps for lithospheric shear zones

Fields for climb-assisted dislocation creep, with stress exponent 3, DRX creep following Eq. (16), and grain-boundary (Coble) diffusion creep, are shown for quartz and olivine on stress/grainsize and stress/temperature maps in Figs. 6 and 7. For simplicity we have not included fields for exponential creep. Strain rates were calculated from the theoretical flow laws, and the boundaries between fields indicate where the strain rates produced by the adjacent deformation mechanisms are equal. The flow laws used and the values of the parameters are given in the Appendix. On the stress/grainsize maps, the grainsize is treated as an independent variable, and the empirical grainsize-stress relationships for quartz and olivine respectively are shown for reference. We constructed the stress/temperature maps assuming that the material obeys the empirical relationships, however, so that the grainsize is a function of stress. Note that on the stress/grainsize maps, the boundary between the climb-assisted dislocation creep and DRX creep fields is only weakly dependent on stress (and therefore very steep), because the stress exponent is the same when D_r is treated as an independent variable; but it is sensitive to temperature, because the activation energies are for self diffusion and grain-boundary diffusion respectively. The temperature sensitivity causes the boundary to move to smaller grainsizes at higher temperatures, and hence to higher stresses at higher temperatures on the stress/temperature map. Because of the uncertainties in the theoretical parameters (see above, and the Appendix), the positions of these boundaries and the values of the strain rates are poorly constrained. They are shown in Figs. 6 and 7 for illustrative purposes only, but the slopes, and hence the overall topology of the diagrams, are reasonably robust.

The empirical piezometer for quartz lies mainly in the DRX creep field shown in Fig. 6. The topology of the map indicates that at lower stresses and larger grainsizes climb-assisted dislocation creep will dominate. Dynamic recrystallization and grainsize reduction in quartz may therefore cause a switch from grainsize-insensitive dislocation creep to grainsize-sensitive DRX creep. This provides a plausible weakening mechanism during the deformation of crustal rocks, and we suggest that most quartz mylonites deform by DRX creep, and that this explains strain localization in the middle crust.

The empirical piezometer for olivine falls in the diffusion creep field except at very high temperatures (Warren and Hirth, 2006), and does not appear to enter the DRX field (Fig. 7). The experimental data were obtained from rocks that deformed by dislocation creep, however. This may reflect problems with extrapolating experimental data for stress/D_r relationship or for flow laws (or both) to geological strain rates and temperatures. Alternatively, various workers have discussed the possibility of a switch in deformation mechanism to diffusion creep induced by dynamic recrystallization (Etheridge and Wilkie, 1979; Rutter and Brodie, 1988). Hirth and Kohlstedt (2003) have also suggested that there may be a grainsize-sensitive deformation field involving grain-boundary sliding accommodated by an additional mechanism (either diffusion or dislocation creep), which could be activated by grainsize reduction. Diffusion creep and grain-boundary sliding do not in themselves modify the grainsize, but in the absence of continued dynamic recrystallization, grains will grow in order to reduce the total surface energy in the system. This inference is supported by experimental data in the diffusion creep field in which the grainsize appears to follow a normal grain growth law (Karato, 1989; Walker et al., 1990). This would cause a reduction in the rate of grainsize-sensitive creep, and bring the material back toward the dislocation creep field. De Bresser et al. (1998) therefore argued that the grainsize would increase until the strain rates accommodated by dislocation creep and by grainsize-sensitive creep were the same, so that the material would lie on the boundary between the two fields, largely counteracting the effect of the deformation mechanism switch.

This possibility has been the subject of much debate. Deformation mechanism switches provides a mechanism for substantial weakening and hence localization of strain, but De Bresser et al. (1998) have suggested that these switches would be counteracted by surface energy driven grain growth in the diffusion creep field. If, as suggested by Platt and Behr (2011), lithospheric-scale shear zones evolve at approximately constant stress, rather than at constant strain-rate, this may not be the case. The microstructural evolution of an initially coarse-grained peridotite, deformed at relatively high stress, is shown for illustration in Fig. 7b. Deformation starts at a grainsize of 1 mm and a stress of 170 MPa (Point A in Fig. 7b). Dynamic recrystallization reduces the grainsize to 18 μm, on the piezometer line (point B). The dominant deformation then switches to diffusion creep. At constant strain-rate, this results in a stress drop, to 10 MPa (point C), where the strain-rate is the same as that initially imposed at A (10^{-9}/sec). The rock then lies below the $D_{\min}$ line, so grain growth can occur, which may bring the rock back toward the field boundary (point D), as proposed by De Bresser et al. (1998). If, on the other hand, deformation is taking place at constant stress, the rock will remain at point B. This will result in a substantial increase of strain-rate, but the flow stress remains the same. As a result, the rate of dislocation creep, the dislocation density in the deforming grains, and the dynamically recrystallized grainsize, will all remain unchanged; but the total strain-rate will be dominated by the much higher rate of diffusion creep. The rate of ρGBM will be much higher than γGBM (the position of the material in stress/grainsize space is well above the

D_{min} line). Hence there will be no surface energy driven grain growth, and the material will continue to deform predominantly by diffusion creep. The same line of reasoning applies to any deformation mechanism switch caused by grainsize reduction at constant stress: the resulting weakening will be permanent, so long as the tectonic boundary conditions remain unchanged. Grainsize reduction caused by dynamic recrystallization may therefore play a fundamental role in localizing zones of high strain, and may be a key process in the maintenance of plate tectonics.

8. Conclusions

Our discussion of the controls of grainsize evolution in deforming rocks leads to several conclusions of importance to research in both rock rheology and geodynamics.

1. Under the high stress and relatively low temperatures characteristic of deformation in the upper half of the lithosphere, grainsize reduction by dynamic recrystallization results in a profound modification of both the microstructure and rheology of rock. Strain energy driven grain-boundary migration (ρGBM) is involved both in the nucleation of new grains by the BLG mechanism, and in the subsequent evolution of the microstructure. Above the D_{min} line, which is a line in stress/grainsize space that defines the minimum possible size of nucleus that can form by BLG, ρGBM dominates the microstructure, and grain growth by surface energy driven grain-boundary migration (γGBM) is inhibited. The grainsize produced by dynamic recrystallization is therefore dominated by the nucleation process.

2. Nucleation by both the SGR and BLG mechanisms is likely to be controlled by the size of subgrains or dislocation cells in the within grains deformed by dislocation creep, and above the D_{min} line, this size will not be significantly modified after nucleation. This provides a first-order explanation for the experimentally observed inverse linear grainsize-stress relationship.

3. ρGBM is an important agent of recovery in rocks deformed by dislocation creep, sweeping out dislocations and counteracting work-hardening. We have derived a new flow law (DRX-assisted dislocation creep) based on this process, which is driven by dislocation motion, but shows grainsize sensitivity as a result of the role of ρGBM. If grainsize obeys the empirically-determined grainsize-stress relationship, DRX creep has an effective stress exponent of a little over 4, consistent with experimental observations and inferences from naturally deformed rocks that suggest an exponent of this magnitude. DRX creep may be an important agent in weakening quartz-rich rocks at low temperatures; current flow law data suggest that it is less likely to be important in olivine-rich rocks.

4. Rocks deformed so that they lie above the D_{min} line in stress/grainsize space are likely to undergo transitions from climb-assisted dislocation creep to grainsize-sensitive creep (Coble creep, DRX creep, or creep dominated by grain-boundary sliding). All these mechanisms result in weakening at low temperature and high stress. If shear zones evolve at constant stress, as suggested by Platt and Behr (2011), then weakening results in an increase in strain rate, due to the contributions of the additional mechanisms. The rate of dislocation motion, the dislocation density, and the dynamically recrystallized grainsize, will remain the same, however. Grain growth will be inhibited by the activity of ρGBM. Hence the deformation mechanism switches and the weakening they cause will be permanent, so long as the tectonic boundary conditions remain unchanged. Grainsize reduction caused by dynamic recrystallization is therefore likely to play a fundamental role in lithospheric weakening, and may be the key process in the maintenance of plate tectonics.

Acknowledgments

This research was supported by NSF grant EAR-0809443 awarded to J.P. Platt. We thank H. de Bresser, I. Shimizu, and M. Stipp for their helpful reviews.

Appendix

The deformation mechanism maps in Figs. 6 and 7 were constructed using theoretical flow laws for climb-controlled dislocation creep, DRX creep, and grain-boundary diffusion creep (Coble creep), as follows. Parameters and their values for quartz and olivine are listed in Table 1.

Following Poirier (1985), the flow law for climb-controlled dislocation creep can be derived from Orowan's equation by including the dimensionless ratio of the glide distance L to the climb distance z:

$$\dot{e} = \rho b \frac{L}{z} v_c \tag{A1}$$

where $z \approx \mu b/2\sigma$ (Karato, p. 158, Eq. (9.56) and $L = g\mu b/\sigma$ is the dislocation path length (Devincre et al., 2008). g is dependent on crystal orientation, and for FCC metals, is in the range 4.6–10.4. The climb velocity v_c is

$$v_c = \frac{\sigma \Omega D_v}{lkT} \tag{A2}$$

where $\Omega = b^3$, D_v is the coefficient for self diffusion, and the length scale l is:

$$l = \frac{b}{2\pi} \ln\left(\frac{1}{2b\sqrt{\rho}}\right) \tag{A3}$$

The dislocation density is related to stress by:

$$\rho = \left(\frac{\sigma}{\alpha \mu b}\right)^2 \tag{A4}$$

With the addition of the water fugacity term, this gives:

$$\dot{e} = \frac{4g\pi b D_v}{\alpha^2 \mu^2 kT \ln(\alpha\mu/2\sigma)} f(H_2O)\sigma^3 \tag{A5}$$

where the coefficient of volume diffusion $D_v = D_{0v}\exp(-Q_v/RT)$.

The flow law for DRX creep is derived in this paper, and we added a water fugacity term:

$$\dot{e} = \frac{C_2 g M \chi \ln(\alpha\mu\beta/2\sigma)}{4\pi\alpha^4\mu^2 D_r} f(H_2O)\sigma^3 \tag{A6}$$

where the grain-boundary mobility $M = bwD_{gb}/kT$, and coefficient of grain-boundary diffusion is $D_{gb} = D_{0gb}\exp(-Q_{gb}/RT)$.

The Coble creep flow law is taken from Poirier (1985):

$$\dot{e} = \frac{42\pi V w D_{gb}\sigma}{RTD_r^3} \tag{A7}$$

The water fugacity f(H_2O) is calculated for "wet" flow laws (including quartz) assuming that the water pressure is equal to lithostatic, using the fugacity calculator at http://www.geo.umn.edu/people/researchers/withe012/fugacity.htm (Pitzer and Sterner, 1994).

For each flow law, a scaling factor was included, which allowed us to benchmark the climb-controlled dislocation creep and diffusion creep flow laws to experimental data. The benchmarking was done as follows.

For climb-controlled dislocation creep in quartz, the scaling factor was used to obtain a strain rate of 3×10^{-5} s^{-1} at 300 MPa fluid pressure, 1200 °C, and 158 MPa differential stress, as obtained by Rutter and Brodie (2004b). Rather than use their value of Q_v (242 kJ mol^{-1}), we used 145 kJ mol^{-1}, similar to the value obtained by Hirth et al. (2001), to obtain a strain rate of $\sim 10^{-13}$ s^{-1} at 300 °C, 150 MPa differential stress, which we think corresponds to natural conditions at the point of initiation of a natural shear zone near the BDT. For DRX creep we chose values that give a strain-rate roughly one order of magnitude faster, reflecting the effect of weakening in mylonite zones. Experimental data for Coble creep in quartz is insufficiently consistent for us to be able to benchmark the theoretical flow law for this process (Rutter and Brodie, 2004a), so we used the same scaling factor as for DRX creep.

For dry climb-assisted dislocation creep in olivine, the scaling factor was used to get a strain rate of 10^{-5} s^{-1} at 300 MPa fluid pressure, 1250 °C, and 200 MPa differential stress, as obtained by Hirth and Kohlstedt (2003). For DRX creep we chose values that give a strain rate about one order of magnitude faster than their dry dislocation creep law at 700 °C. For diffusion creep we used a scaling factor that gives similar strain rates to the dry diffusion creep law of Hirth and Kohlstedt (2003).

The scaling factors serve to bring the theoretical flow laws into line with the experimental laws. A factor of $\sim 10^6$ results from our inclusion of a water fugacity term with numerical value of order 10^2 representing the H/Si ratio, which has a numerical value of order 10^{-4}. Other contributing factors are likely to arise from uncertainties on many of the parameters listed in Table 1. In view of this, the strain rates and deformation mechanism boundaries shown in Figs. 6 and 7 should be regarded as illustrative in nature only. The topology of the maps is, we believe, robust.

References

Austin, N.J., Evans, B., 2007. Paleowattmeters: a scaling relation for dynamically recrystallized quartz grains. Geology 35, 343–346.

Behr, W.M., Platt, J.P., 2011. A naturally constrained stress profile through the middle crust in an extensional terrane. Earth and Planetary Science Letters. doi:10.1016/j.epsl.2010.11.044.

Bercovici, D., 2003. The generation of plate tectonics from mantle convection. Earth and Planetary Science Letters 205, 107–121.

Berman, R.G., 1988. Internally-consistent thermodynamic data for minerals in the system Na2O–K2O–CaO–MgO–FeO–Fe2O3–Al2O3–SiO2–TiO2–H2O–CO2. Journal of Petrology 29, 455–522.

Brady, J.B., 1994. Diffusion data for silicate minerals, glasses, and liquids. In: Mineral Physics and Crystallography – A Handbook of Physical Constants. American Geophysical Union, Washington, D.C, pp. 269–290.

Braun, J., Chéry, J., Poliakov, A., Mainprice, D., Vauchez, A., Tomassi, A., Daignières, M., 1999. A simple parameterization of strain localization in the ductile regime due to grainsize reduction: a case study for olivine. Journal of Geophysical Research 104, 25167–25181.

Brodie, K.H., Rutter, E.H., 1987. The role of transiently fine-grained reaction products in syntectonic metamorphism: natural and experimental examples. Canadian Journal of Earth Sciences 24, 556–564.

Burke, J.E., Turnbull, D., 1952. Recrystallization and grain growth. Progress in Metal Physics 3, 220–292. doi:10.1016/0502-8205(52)90009-9.

De Bresser, J.H.P., Peach, C.J., Reijs, J.P.J., Spiers, C.J., 1998. On dynamic recrystallization during solid state flow: effects of stress and temperature. Geophysical Research Letters 25, 3457–3460.

De Bresser, J.H.P., Ter Heege, J.H., Spiers, C.J., 2001. Grainsize reduction by dynamic recrystallization: can it result in major rheological weakening? International Journal of Earth Sciences 90, 28–45.

Derby, B., 1991. The dependence of grainsize on stress during dynamic recrystallization. Acta Metallurgica and Materialia 39, 955–962.

Derby, B., 1992. Dynamic recrystallization: the steady state grainsize. Scripta Metallurgica et Materialia 27, 1581–1586.

Derby, B., Ashby, M.F., 1987. On dynamic recrystallization. Scripta Metallurgica 21, 879–884.

Devincre, B., Hoc, T., Kubin, L., 2008. Dislocation mean free paths and strain hardening of crystals. Science 320, 1745–1748.

Dolmen, R., Chakraborty, S., Becker, H.W., 2002. Si and O diffusion in olivine and implications for characterizing plastic flow in the mantle. Journal of Geophysical Research 29, 2030. doi:10.1029/2002GL015480.

Drury, M.R., 2005. Dynamic Recrystallization and Strain Softening of Olivine Aggregates in the Laboratory and the Lithosphere. In: Geological Society of London Special Publication, vol. 243 127–142.

Dunlap, W.J., Hirth, G., Teyssier, C., 1997. Thermomechanical evolution of a ductile duplex. Tectonics 16, 983–1000.

Duyster, J., Stockhert, B., 2001. Grain boundary energies in olivine derived from natural microstructures. Contributions to Mineralogy and Petrology 140, 567–576.

Etheridge, M.A., Wilkie, J.C., 1979. Grainsize reduction, grain boundary sliding and the flow strength of mylonites. Tectonophysics 58, 159–178.

Evans, B., Renner, J., Hirth, G., 2001. A few remarks on the kinetics of static grain growth in rocks. International Journal of Earth Sciences 90, 80–103.

Farver, J.R., Yund, R.A., 2000a. Silicon diffusion in a natural quartz aggregate: constraints on solution-transfer diffusion creep. Tectonophysics 325, 193–205.

Farver, J.R., Yund, R.A., 2000b. Silicon diffusion in forsterite diffusion accommodated creep. Geophysical Research Letters 27, 2337–2340.

Fliervoet, T.F., White, S.H., 1995. Quartz deformation in a very fine-grained quartzofelspathic mylonite: a lack of evidence for dominant grain-boundary sliding deformation. Journal of Structural Geology 17, 1095–1111.

Hall, C.E., Parmentier, E.M., 2003. Influence of grainsize evolution on convective instability. Geochemistry, Geophysics, Geosystems 4, 1029. doi:10.1029/2002GC000308.

Handy, M., Hirth, G., Bürgmann, R., 2007. Continental fault structure and rheology from the frictional-to-viscous transition downward. In: Handy, M., Hirth, G., Hovius, N. (Eds.), Tectonic Faults: Agents of Change on a Dynamic Earth. The MIT Press., Cambridge, Mass.

Hiraga, T., Nishikawa, O., Nagase, T., Akizuki, M., Kohlstedt, D., 2007. Interfacial energies for quartz and albite in pelitic schist. Contributions to Mineralogy and Petrology 143, 664–672. doi:10.1007/s00410-002-0375-4.

Hirth, G., Kohlstedt, D., 2003. Rheology of the upper mantle and the mantle wedge: a view from the experimentalists. Geophysical Monograph. In: Inside the Subduction Factory, vol. 138. American Geophysical Union, pp. 83–105.

Hirth, G., Tullis, J., 1992. Dislocation creep regimes in quartz aggregates. Journal of Structural Geology 14, 145–160.

Hirth, G., Teyssier, C., Dunlap, W.J., 2001. An evaluation of quartzite flow laws based on comparisons between experimentally and naturally deformed rocks. International Journal of Earth Sciences 90, 77–87. doi:10.1007/s005310000152.

Holland, T., Powell, R., 1998. An internally consistent thermodynamic data set for phases of petrological interest. Journal of Metamorphic Geology 16, 309–344.

Holyoke, C.W., Kronenberg, A.K., 2010. Accurate differential stress measurement using the molten salt cell and solid salt assemblies in the Griggs apparatus with applications to strength, piezometers and rheology. Tectonophysics 494, 17–31. doi:10.1016/j.tecto.2010.08.001.

Humphreys, F.J., Hatherly, M., 2004. Recrystallization and Related Annealing Phenomena. Elsevier Science Ltd, Oxford, UK.

Jaroslow, G.E., Hirth, G., Dick, H.J.B., 1996. Abyssal peridotite mylonites: implications for grain-size sensitive flow and strain localization in the oceanic lithosphere. Tectonophysics 256, 17–37.

Jessell, M.W., 1987. Grain-boundary migration microstructures in a naturally deformed quartzite. Journal of Structural Geology 9, 1007–1014.

Jin, D., Karato, S.-I., Obata, M., 1998. Mechanisms of shear localization in the continental lithosphere: inference from the deformation microstructures of peridotites from the Ivrea Zone, northwestern Italy. Journal of Structural Geology 20, 195–210.

Karato, S., 1989. Grain growth kinetics in olivine aggregates. Tectonophysics 168, 255–273.

Karato, S., Wu, J., 1993. Rheology of the upper mantle: a synthesis. Science 260, 771–772.

Kohlstedt, D.L., Weathers, M.S., 1980. Deformation-induced microstructures, paleopiezometers, and differential stresses in deeply eroded fault zones. Journal of Geophysical Research 85, 6269–6285.

Montési, L.G.J., Hirth, G., 2003. Grainsize evolution and the rheology of ductile shear zones: from laboratory experiments to postseismic creep. Earth and Planetary Science Letters 211, 97–110. doi:10.1016/S0012-821X(03)00196-1.

Montési, L.G.J., Zuber, M.T., 2002. A unified description of localization for application to large-scale tectonics. Journal of Geophysical Research 107. doi:10.1029/2001JB000465.

Parks, G.A., 1984. Surface and interfacial energies of quartz. Journal of Geophysical Research 89, 3997–4008.

Pitzer, K.S., Sterner, S.M., 1994. Equations of state valid continuously from zero to extreme pressures for H2O and CO2. Journal of Chemical Physics 101, 3111–3116.

Platt, J.P., Behr, W.M., 2011. Lithospheric shear zones as constant stress experiments. Geology 39, 127–130. doi:10.1130/G31561.1.

Poirier, J.-P., 1985. Creep of Crystals. Cambridge University Press, Cambridge, UK.

Poirier, J.P., 1980. Shear localization and shear instability in materials in the ductile field. Journal of Structural Geology 2, 135–142.

Precigout, J., Gueydan, F., Gapais, D., Garrido, C.J., Essaifi, A., 2007. Strain localisation in the subcontinental mantle — a ductile alternative to the brittle mantle. Tectonophysics 445, 318–336.

Regenauer-Lieb, K., Weinberg, R.F., Rosenbaum, G., 2006. The effect of energy feedbacks on continental strength. Nature 442, 67–70. doi:10.1038/nature04868.

Ross, J.V., Avé Lallemant, H.G., Carter, N.L., 1980. Stress dependence of recrystallized grain and sub-grainsize in olivine. Tectonophysics 70, 39–61.

Rutter, E.H., 1995. Experimental study of the influence of stress, temperature, and strain on the dynamic recrystallization of Carrara marble. Journal of Geophysical Research 100, 24651–24663.

Rutter, E.H., Brodie, K.H., 1988. The role of tectonic grainsize reduction in the rheological stratification of the lithosphere. Geologische Rundschau 77, 295–308.

Rutter, E.H., Brodie, K.H., 2004a. Experimental grain-size sensitive flow of hot-pressed Brazilian quartz aggregates. Journal of Structural Geology 26, 2011–2024.

Rutter, E.H., Brodie, K.H., 2004b. Experimental intracrystalline plastic flow in hot-pressed synthetic quartzite prepared from Brazilian quartz crystals. Journal of Structural Geology 26, 259–270. doi:10.1016/S0191-8141(03)00096-8.

Sakai, T., 1989. Dynamic recrystallization of metallic materials. In: Karato, S., Toriumi, M. (Eds.), Rheology of Solids and of the Earth. Oxford University Press, Oxford, UK, pp. 284–307.

Schmid, S.M., Paterson, M.S., Boland, J.N., 1980. High temperature flow and dynamic recrystallization in Carrara marble. Tectonophysics 65, 245–280.

Shimizu, I., 1998. Stress and temperature dependence of recrystallized grainsize: a subgrain misorientation model. Geophysical Research Letters 25, 4237–4240.

Shimizu, I., 2008. Theories and applicability of grainsize piezometers: the role of dynamic recrystallization mechanisms. Journal of Structural Geology 30, 899–917.

Stipp, M., Kunze, K., 2008. Dynamic recrystallization near the brittle-plastic transition in naturally and experimentally deformed quartz aggregates. Tectonophysics 448, 77–97. doi:10.1016/j.tecto.2007.11.041.

Stipp, M., Stünitz, H., Heilbronner, R., Schmid, S.M., 2002a. Dynamic Recrystallization of Quartz: Correlation Between Natural and Experimental Conditions. In: Geological Society of London Special Publication, vol. 200 171–190.

Stipp, M., Stünitz, H., Heilbronner, R., Schmid, S.M., 2002b. The eastern Tonale fault zone: a 'natural laboratory' for crystal plastic deformation of quartz over a temperature range from 250–700 °C. Journal of Structural Geology 24, 1861–1884.

Stipp, M., Tullis, J., 2003. The recrystallized grainsize piezometer for quartz. Geophysical Research Letters 30, 2088. doi:10.1029/2003GL018444.

Stipp, M., Tullis, J., Scherwath, M., Behrmann, J.H., 2010. A new perspective on paleopiezometry: dynamically recrystallized grainsize distributions indicate mechanism changes. Geology 38, 759–762. doi:10.1130/G31162.1.

Tackley, P.J., 2000. Mantle convection and plate tectonics: toward and integrated physical and chemical theory. Science 288, 2002–2007.

Tingle, T.N., Green, H.W., Scholz, C.H., Koczynski, T.A., 1993. The rheology of faults triggered by the olivine-spinel transformation in Mg2GeO4 and its implications for the mechanism of deep-focus earthquakes. Journal of Structural Geology 15, 1249–1256.

Trompert, R., Hansen, U., 1998. Mantle convection simulations with rheologies that generate plate-like behaviour. Nature 395, 686–689.

Tullis, J., Yund, R., Farver, J., 1996. Deformation enhanced fluid distribution in feldspar aggregates and implication for ductile shear zones. Geology 24, 63–66.

Tullis, J., Yund, R.A., 1982. Grain-growth kinetics of quartz and calcite aggregates. Journal of Geology 90, 301–318.

Tullis, J., Yund, R.A., 1985. Dynamic recrystallization of feldspar: a mechanism for ductile shear zone formation. Geology 13, 238–241.

Twiss, R.J., 1977. Theory and applicability of a recrystallized grainsize paleopiezometer. Pure and Applied Geophysics 115, 227–244.

van der Wal, D., Chopra, P., Drury, M., Fitz Gerald, J., 1993. Relationship between dynamically recrystallized grainsize and deformation conditions in experimentally deformed olivine rocks. Geophysical Research Letters 20, 1479–1482.

Walker, A., Rutter, E.H., Brodie, K.H., 1990. Experimental Study of Grain-size Sensitive Flow of Synthetic, Hot-pressed Calcite Rocks. In: Geological Society of London Special Publication, vol. 54 259–284.

Warren, J.M., Hirth, G., 2006. Grainsize sensitive deformation mechanisms in naturally deformed peridotites. Earth and Planetary Science Letters 248, 438–450. doi:10.1016/j.epsl.2006.06.006.

White, S., 1976. The effects of strain on the microstructures, fabrics and deformation mechanisms in quartzites. Philosophical Transactions of the Royal Society 283A, 69–86.

White, S.H., Knipe, R.J., 1978. Transformation-and reaction-enhanced ductility in rocks. Journal of the Geological Society, London 135, 513–516.

Zhong, S., Gurnis, M., 1996. Interaction of weak faults and non-Newtonian rheology produces plate tectonics in a 3D model of mantle flow. Nature 383, 245–247.